Supporting Information

3D-printed framework with gradient distributed heterojunction and fast Li^+ conductivity interfaces for high-rate lithium metal anodes

Shuo Wang[a], Haiting Shi[a]*, Yuanhua Xia[b], Dong Liu[b], Chunying Min[c], Ming Zeng[a], Sirui Liang[a], Ruiqi Shao[a], Xiaoqing Wu[a], Zhiwei Xu[a]*

[a]State Key Laboratory of Separation Membranes and Membrane Processes, School of Textile Science and Engineering, Tiangong University, Tianjin, China, 300387

[b]Key Laboratory of Neutron Physics, Institute of Nuclear Physics and Chemistry, China Academy of Engineering Physics, Mianyang, China, 621999

[c]Research School of Polymeric Materials, School of Materials Science & Engineering, Jiangsu University, Zhenjiang, Jiangsu, China, 212013

Nanoindentation experiment

The nanoindentation experiment was completed by Nanoindenter XP (Hysitron TI 980 TriboIndenter, Germany) with a diamond (Berkovich) indenter. The constant loading rate (dP/dt as a constant) mode is used in the stiffness test of the sample. The sample test process is followed by loading for 20 s, holding for 15 s, unloading to 10% of the maximum load, and holding for 60 s. The hardness H is calculated by the O&P method.

DFT calaulation

On the basis of the density functional theory (DFT), all calculations were performed by spin-polarized version of Vienna ab initio simulation package (VASP) in Mede A software. The projected augmented wave method (PAW) was adopted to describe the

* Corresponding author. E-mail address: shihaiting@tiangong.edu.cn (Haiting Shi); xuzhiwei@tiangong.edu.cn (Zhiwei Xu)

electron-ion interactions. The Perdue–Burke–Ernzerhof (PBE) version of the generalized gradient approximation (GGA) was used for exchange-correlation potentials. DFT-D2 method of Grimme was employed to correctly describe van der Waals interactions. The cutoff energy for plane wave basis was set to be 400 eV, which was sufficient for a good energy convergence. The conjugate gradient method scheme was applied for the structural optimization with the convergence criterion of energy in 10^{-5} eV and of force on each atom in 0.02 eV $Å^{-1}$. To eliminate the interactions between the separated nanosheets, a vacuum space of 15 Å was set in c direction with the periodic boundary conditions in a and b directions. The corresponding Brillouin zone integration was carried out using 3×3×1 k-point meshes by Monkhorst–Pack scheme.

Table S1 Electronic conductivity of different sides of 3D frameworks

Times	Top side (S m^{-1})	Bottom side (S m^{-1})
1	3.15	1.75
2	2.59	2.17
3	2.96	2.34

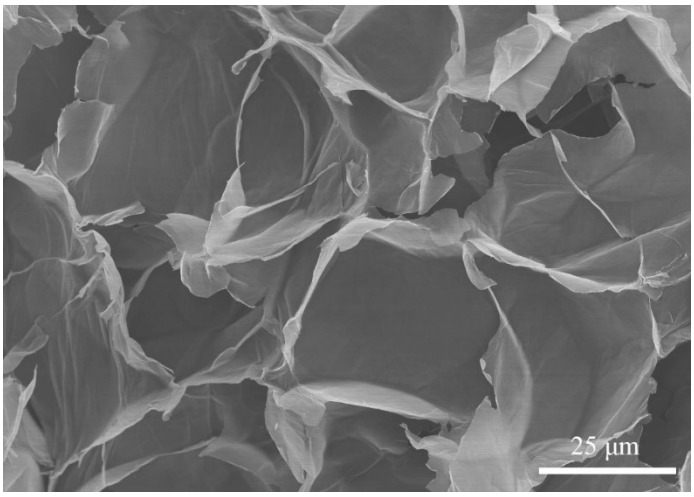

Figure S1 Side views for the top section without γ-Al_2O_3.

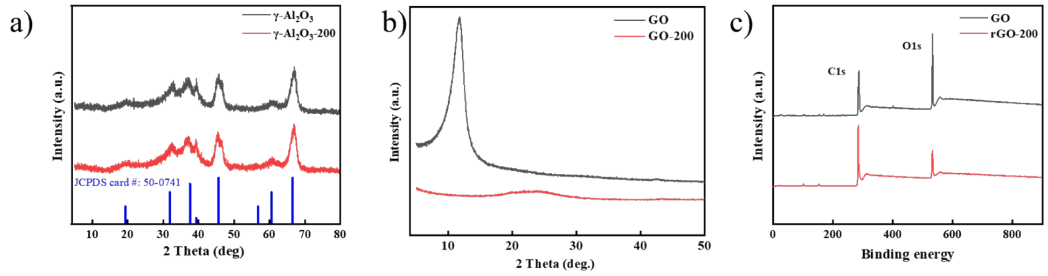

Figure S2 a) XRD patterns of pristine γ-Al_2O_3 and annealing γ-Al_2O_3. b) XRD patterns of GO and GO-200. b) XPS patterns of GO and annealing GO.

Table S2 Chemical composition of samples determined from XPS spectra

Samples	Element content (at%)		% of total C1s			
	C	O	C=C	C-C/C-N	C-O	O=C-O
GO	67.3	32.7	29.8	17.3	43.3	9.6
GO-200	79.5	20.5	51.9	29.4	4.6	14.1

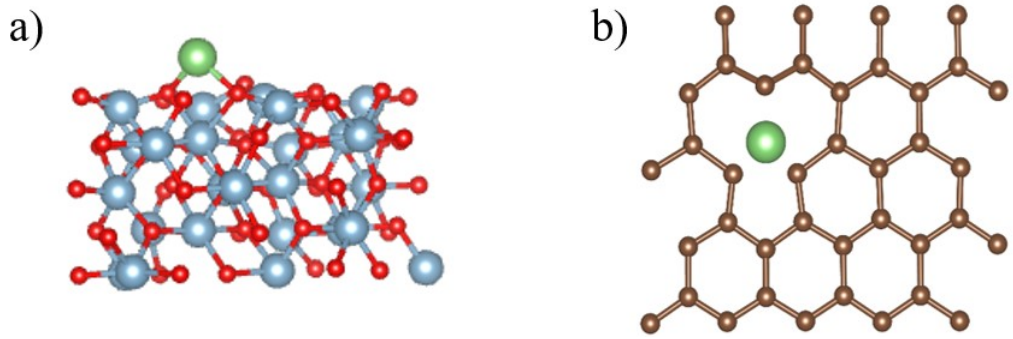

Figure S3 calculation model of a) γ-Al_2O_3 and b) graphene with two atomic defects.

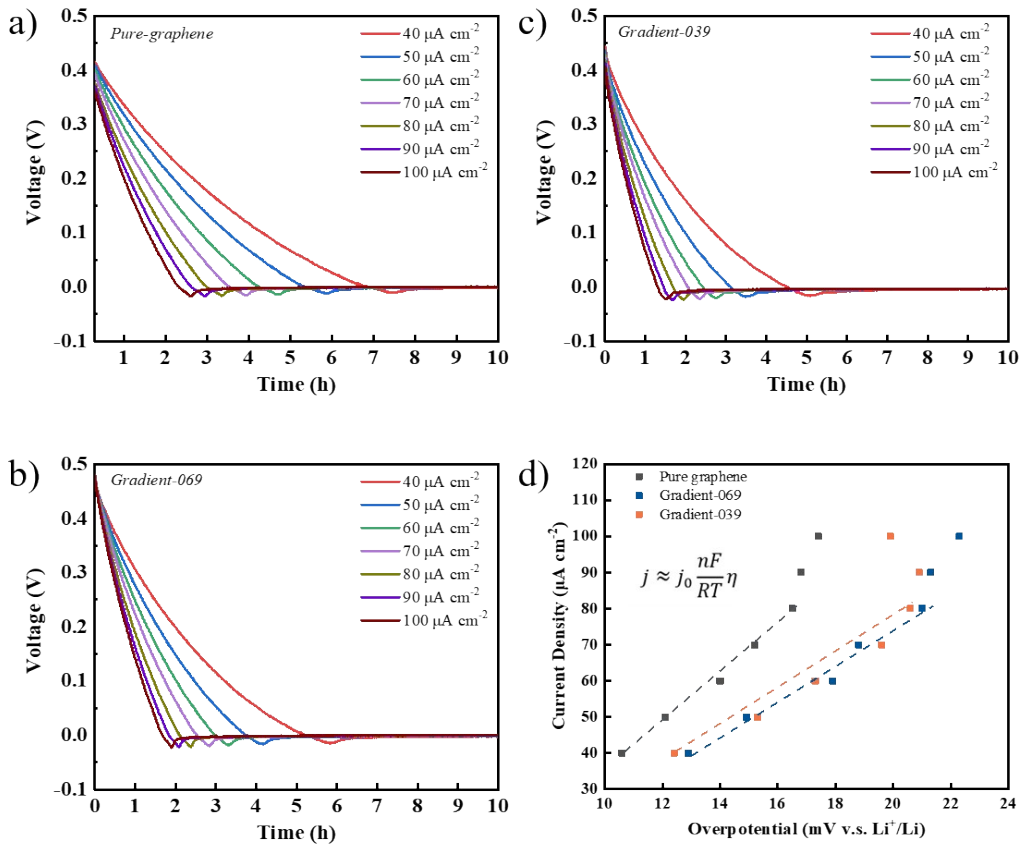

Figure S4 a-c) The overpotential (η) at different current densities (j) for three types of frameworks. d) The relationship between overpotential (η) and current densities (j).

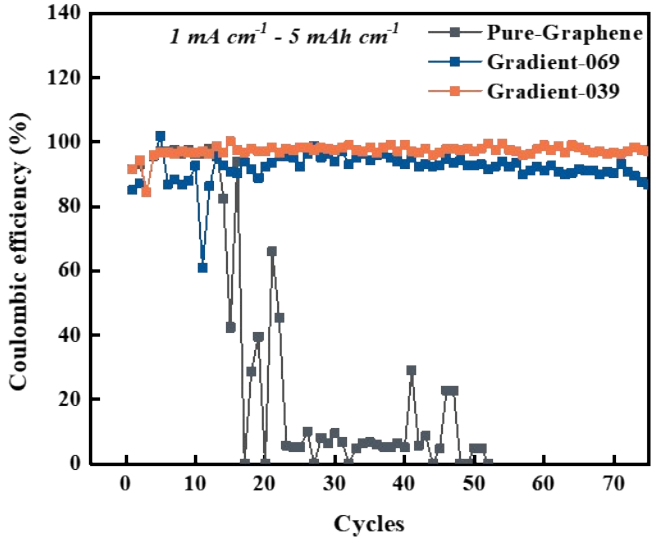

Figure S5 a) Coulombic efficiency of 3D frameworks at 1 mA cm^{-2} for 5 mAh cm^{-2}.

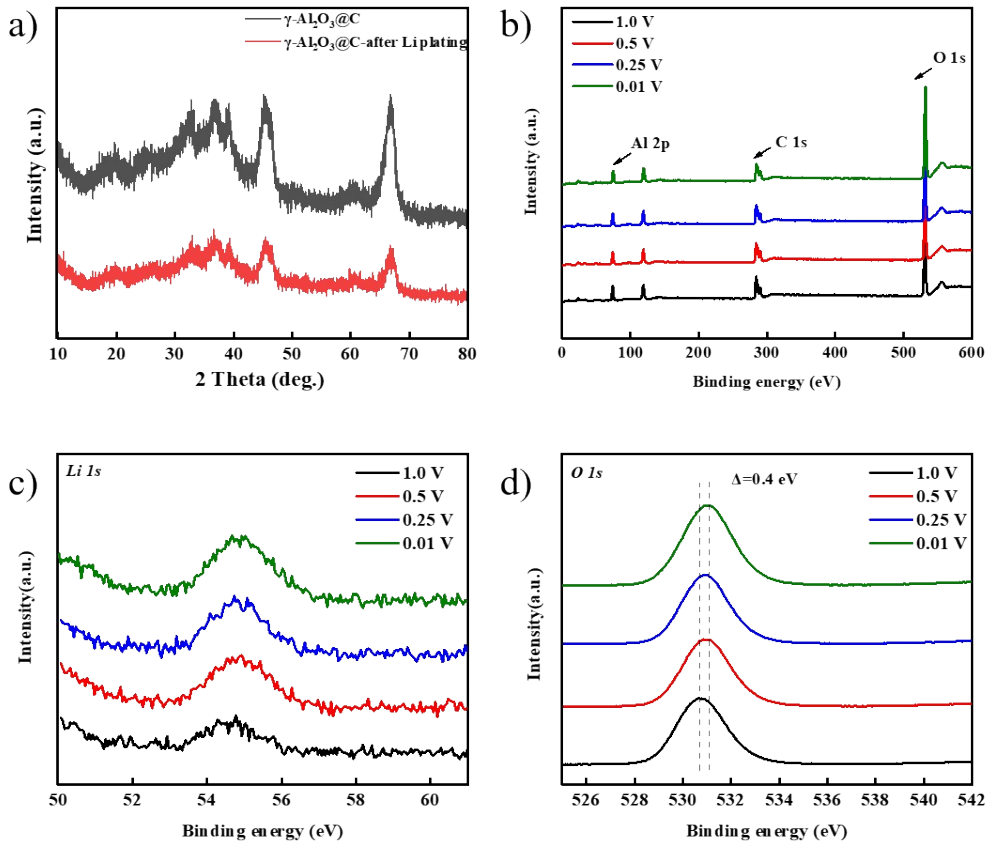

Figure S6 a) XRD patterns of the γ-Al_2O_3@graphene slurry electrode before and after 1 mAh cm^{-2} Li plating. b) XPS patterns of the γ-Al_2O_3@graphene slurry electrode with different depth of discharge. c-d) Li 1s and O 1s spectra with different depth of discharge.

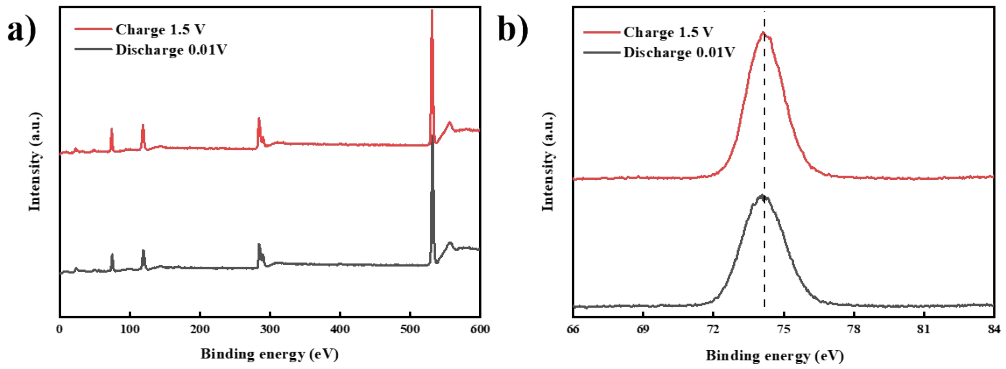

Figure S7, a) XPS patterns of the γ-Al_2O_3@graphene slurry electrode with discharge to 0.01V and charge to 1.5 V. b) The Al 2p XPS spectra of the slurry electrode with

discharge to 0.01V and charge to 1.5 V

Table S3 Latest cycle stability of lithium metal batteries and full cells.

Materials	Cycle stability in symmetrical cells	Full cell performance (LFP cathode)	Ref.
3D flexible MXene@Au host	650 hours at 1 mA cm^{-2}, 1 mAh cm^{-2}	131.41 mAh g^{-1} at 1 C with a high capacity retention rate of 98.47%.	1
Ultrafine TiO_2 confined in 3D freestanding carbon paper	550 hours at 0.5 mA cm^{-2}, 0.5 mAh cm^{-2}	An initial capacity of 128 mAh g^{-1} after 250 cycles with 99.2% Coulombic efficiency.	2
Multifunctional SnSe–C composite modified 3D scaffolds	1100 hours at 1 mA cm^{-2}, 1 mAh cm^{-2}	A discharge capacity of 102.7 mAh g^{-1} at 2 C rate and still retains 87.2 mAh g^{-1} after 750 cycles.	3
Conformal coating of lithium-zinc alloy on 3D conducting scaffold	400 hours at 1 mA cm^{-2}, 1 mAh cm^{-2}	A high capacity of 145.2 mAh g^{-1} after 150 cycles at 0.2 C	4
MnO_2 Nanoflower Arrays@Ni Foam	2000 hours at 1 mA cm^{-2}, 1 mAh cm^{-2}	A capacity of 138.8 mAh g^{-1} and retains a high capacity retention of 81.2% over 800 cycles at 2 C.	5
lithiophilic 3D skeleton via a versatile MOF-derived route	1000 hours at 2 mA cm^{-2}, 1 mAh cm^{-2}	~140 mAh g^{-1} after 400 cycles at 1 C	6
3D-printed gradient framework	1500 hours at 1 mA cm^{-2} and 1 mAh cm^{-2}	A reversible capacity of 176.8 mAh g^{-1} at 0.5 C deceased to 130.8 mAh g^{-1} at 5 C and capacity retention of 98% after 50 cycles under 0.5 C after rate performance.	This work

References

1. Y. Qian, C. Wei, Y. Tian, B. Xi, S. Xiong, J. Feng and Y. Qian, *Chem. Eng. J.*, 2021, **421**, 129685.
2. Y. Tian, Y. An, C. Wei, Y. Tao, Y. Zhang, H. Jiang, L. Tan, J. Feng and Y. Qian, *Chem. Eng. J.*, 2021, **406**, 126836.
3. X. Shen, G. Zhao, X. Yu, H. Huang, M. Wang and N. Zhang, *J. Mater. Chem. A*, 2021, **9**, 21695-21702.
4. H. Song, T. He, J. Liu, Y. Wang, X. L. Li, J. Liu, D. Zhang, H. Y. Yang, J. Hu and S. Huang, *Carbon*, 2021, **181**, 99-106.
5. Y. Fan, H. Li, X. He, Y. Huang, C. Sun, T. Zhu, H. Liu, E. Huangzhang, F. Sun and J. Nan, *ACS Appl. Energy Mater.*, 2022, **5**, 10034-10044.
6. L. Zeng, T. Zhou, X. Xu, F. Li, J. Shen, D. Zhang, J. Liu and M. Zhu, *Science China Materials*, 2022, **65**, 337-348.